

A study about size effects of 3D periodic cellular structures

L. Yang*

*Department of Industrial Engineering, University of Louisville, Louisville, KY 40292

Abstract

In the design of unit cell based cellular structures, idealized boundary conditions are often assumed to simplify analysis. However, such treatments also result in various deviations from reality. In this study, both lateral and along-the-stress size effects of multiple cellular structural designs under compressive stress with constrained boundary motion were investigated using simulations. It was found that different unit cell designs exhibit significantly different size effects, which might be affected by the unit cell dimensional aspect ratio, the unit cell Poisson's ratios and the unit cell orientations. This study provides a glimpse into the design considerations associated with such phenomenon.

Keywords: Cellular structures, size effects, simulation

Introduction

Unit cell design approach is often employed in the design of 3D non-stochastic cellular structures [1-5]. Using unit cell design, the 3D non-stochastic cellular structures that exhibit geometrical periodicity are treated as spatial patterns of simplified unit geometries and subsequently analyzed. Fig.1 shows some 3D cellular structures and their unit cell geometries. The simplification of the structures enables modeling and analysis of cellular designs with significantly reduced computational costs, which in turn makes it possible to realize more integrated design objectives with lightweight structures [6-9]. In addition, with complete control of geometries, such approach also allows for the design of spatial orientations of individual struts, which is advantageous for additively manufactured materials that exhibit anisotropy.

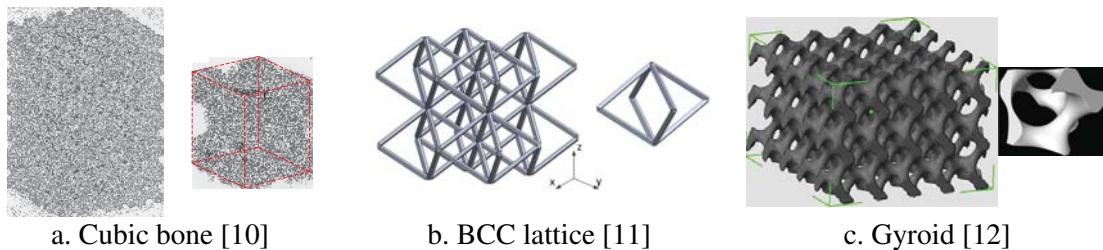


Fig.1 Examples of 3D non-stochastic cellular structures

However, the modeling of unit cell structures imposes multiple assumptions that could potentially introduce errors into the designs [8]. For example, in order to ensure that the loading conditions of a single unit cell are representative to the entire structure, it must be assumed that the structure is subjected to remote stresses and that the boundary constraints can be ignored. However, as actual structures always have finite dimensions and therefore deviate from this condition, size effects occur with cellular structures. Both experimental and modeling based size effect studies have been reported for various cellular structures [13-19]. It was generally observed that both elastic modulus and strength of the cellular

structures increase with increasing number of unit cells in the structures until this number reaches 8-12 depending on the actual cellular geometry. From previous literatures, cellular structure size effects could be categorized into lateral size effects and along-the-stress size effects as shown in Fig.2. Lateral size effects evaluate the influence of lateral free surface on the mechanical properties of structures, and along-the-stress size effects evaluate the influence of boundary constraints (i.e. fixed boundaries) on the mechanical properties of structures. Onck et al. [17] modeled the lateral size effects with 2.5D honeycomb cellular structures, and concluded that the size effect diminishes when the number of unit cell approaches 10, which was subsequently verified experimentally [14]. Tekoglu and Onck [18] studied the along-the-stress size effects of both 2D honeycomb and Voronoi cellular structures, and found that the size effects diminish unit cell number to be around 8. In most of these works, the cellular structures were treated as semi-infinite structures that have no boundary constraints in the directions perpendicular to the ones of interest, which enables the investigation of unidirectional size effects that could be more easily integrated into the unit cell models.

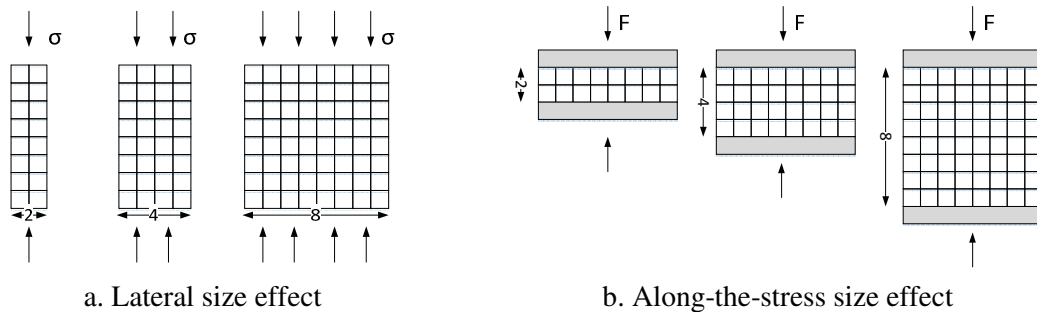


Fig.2 Two types of size effects

However, with actual structures the number of unit cells are often limited in all directions, which result in significantly different boundary conditions that might cause additional stress concentration and structural deformation. Very little works are currently available in the study of coupled effect between lateral and along-the-stress size effects. Therefore, in this work, a simulation based study was carried out to investigate the impact of coupled size effects on elastic mechanical properties of cellular structures.

Design of cellular structures

Four different types of cellular structures were studied, including the re-entrant auxetic structure, the octet-truss structure, the BCC lattice structure, and the rhombic structure, which are shown in Fig.3. All four cellular designs have been designed and realized via additive manufacturing (AM) and studied for mechanical properties [1, 3-5, 11, 19-21]. These cellular designs were selected to investigate the potential relationship between size effects and other cellular design variables such as Poisson's ratios, deformation mechanisms and structural complexity. Among these designs, the re-entrant auxetic structure exhibits negative Poisson's ratios in all three principal directions, the octet-truss structure exhibits high modulus and stretch-dominated deformation [7], while the BCC lattice and rhombic structures both exhibit bending-dominated deformation while having different level of structural complexity. The typical geometrical design parameters of each

type of cellular structures are shown in Fig.3. Note that the cross sectional design parameters are not shown. In this study, square cross sections with dimension t were used for all cellular designs.

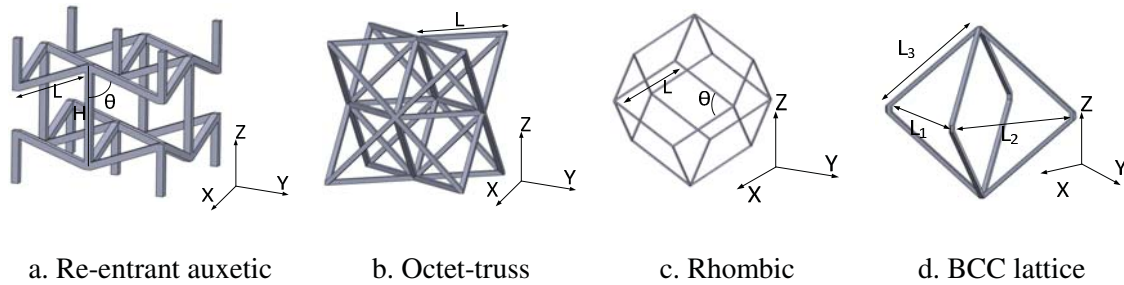


Fig.3 Unit cell designs in current study

All four cellular designs in the current study have cubic geometric bounding volume (GBV), therefore exhibit three principal directions along which the structures can be patterned. Different cellular designs exhibit varying levels of geometrical symmetry and therefore different anisotropic characteristics. For example, re-entrant auxetic structure, the x and y directions as shown in Fig.3 are geometrically identical, therefore the structure exhibits two distinct types of mechanical properties along the x/y and z directions. Similarly, octet-truss structure exhibits identical mechanical properties along the $x/y/z$ directions, rhombic structure exhibits two types of mechanical properties along the x/y and z directions, and the BCC lattice exhibits up to three types of mechanical properties in x, y, z directions depending on the actual designs of its geometrical parameters (L_1, L_2 and L_3). Therefore, the size effects of each cellular structures along these directions will be investigated. It is noted that for BCC lattice the investigation focused on the aspect ratio of the unit cell since all three principal directions are topologically identical.

Table 1 shows the geometrical designs of all the unit cells. For all the unit cell designs, the cross sectional thickness t was set to be 0.8mm. The relative densities of the resulting cellular structures vary between 0.16-0.18 due to the use of “whole” struts at the boundaries during the modeling. However the relative density differences were expected to be negligible for this study, which allows for the investigation to focus on geometrical designs and size effects.

Design	H (L_1)	L (L_2)	θ (L_3)	Relative density
Auxetic 1 (Aux1)	4.2mm	3.6mm	70°	0.16-0.17
Auxetic 2 (Aux2)	7mm	3.5mm	50°	0.16-0.18
Rhombic 1 (Rhomb1)		2.8mm	70°	0.17-0.18
Rhombic 2 (Rhomb2)		3.2mm	100°	0.16-0.17
Octet-truss 1 (Oct1)		5mm		0.18-0.19
BCC-1	3.3mm	6.6mm	4.46mm	0.16-0.17
BCC-2	4.6mm	4.6mm	3.98mm	0.16-0.17

Table 1 Geometrical designs for unit cells

In order to evaluate the size effects, for each cellular design, spatial patterns of 2, 4, 8 unit cells in both lateral and along-the-stress directions were created under every loading cases. An example for the auxetic 1 design is shown in Fig.4.

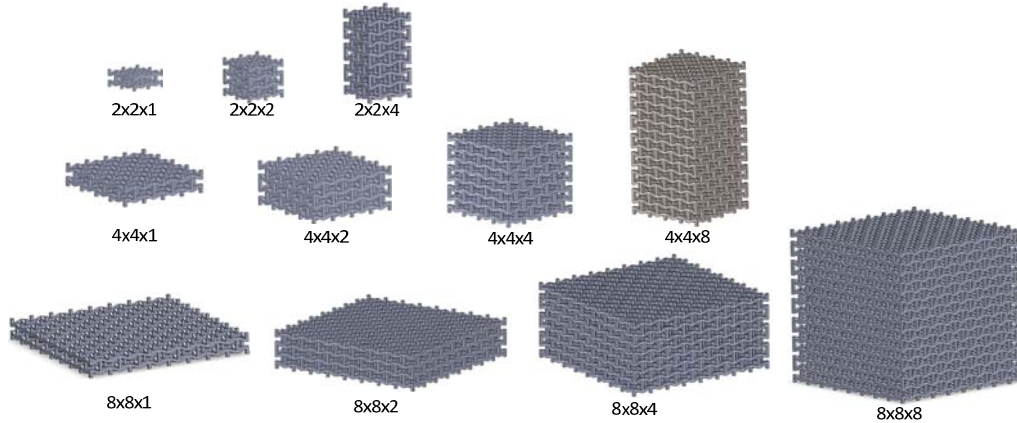


Fig.4 Example of model design for size effect evaluation

The simulations were carried out in SolidWorks Simulation. Although this simulation module does not provide comprehensive finite element analysis capabilities, it provides adequate accuracy in simulating static elastic problems and is also relatively convenient to use. For all simulations, the boundary conditions as shown in Fig.5 were set up. Two rigid blocks were modeled at both ends along the loading directions for the cellular structures, and subsequently used as loading platens. Fully bonded conditions were defined between the cellular structures and the rigid platens in order to simulate completely constrained boundary conditions. The meshing was carried out with the default tetrahedron element with element size of 0.5-0.6mm. It was expected that such rather coarse meshing might introduce inaccuracies, however it was determined that such meshing was preferred due to two reasons. Firstly, the computational costs with finer meshing sizes was found to be inefficient for the computer used for the research. Secondly, coarse meshing was considered adequate to reveal essential size effect information for this study.

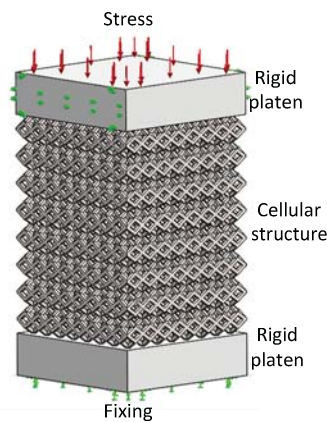


Fig.5 Finite element simulation of cellular structures

As shown in Fig.5, one rigid platen was completely fixed during the simulations, and a 1MPa stress was applied to the other side of the rigid platen along the normal direction. Additional zero displacement constraints were added to some models with large overall aspect ratios to minimize skew errors introduced by simulation tolerances. In addition, the mechanical properties of the single unit cells for each geometrical design and loading

condition combinations were also simulated as used as references. Ti6Al4V was assigned as the material but an arbitrary selection would suffice for the purpose of this study. After the simulation, the elastic modulus of the structures and the maximum Von Mises stress levels were obtained, and the results were compiled for analysis.

Results and Discussions

The size effects of re-entrant cellular structures are shown in Table 2 and Fig.6. E_s and σ_U are the elastic modulus and ultimate strength of Ti6Al4V, and were taken as 104.8GPa and 980MPa.

Design	Pattern (X,Y,Z)	Loading dir.	Normalized elastic modulus (E/E_s)	Normalized max. stress (σ/σ_U)	Design	Pattern (X,Y,Z)	Loading dir.	Normalized elastic modulus (E/E_s)	Normalized max. stress (σ/σ_U)
Aux1	2x2x1	Z	0.00088	0.0735	Aux2	2x2x1	Z	0.00219	0.0461
Aux1	2x2x2	Z	0.00087	0.0731	Aux2	2x2x2	Z	0.00217	0.0475
Aux1	2x2x4	Z	0.00086	0.0727	Aux2	2x2x4	Z	0.00205	0.0477
Aux1	4x4x1	Z	0.00104	0.0865	Aux2	4x4x1	Z	0.00244	0.0532
Aux1	4x4x2	Z	0.00098	0.0873	Aux2	4x4x2	Z	0.00233	0.0544
Aux1	4x4x4	Z	0.00095	0.0861	Aux2	4x4x4	Z	0.00228	0.0544
Aux1	4x4x8	Z	0.00093	0.0860	Aux2	4x4x8	Z	0.00227	0.0518
Aux1	8x8x1	Z	0.00117	0.0842	Aux2	8x8x1	Z	0.00269	0.0538
Aux1	8x8x2	Z	0.00108	0.0939	Aux2	8x8x2	Z	0.00248	0.0657
Aux1	8x8x4	Z	0.00100	0.0934	Aux2	8x8x4	Z	0.00235	0.0690
Aux1	8x8x8	Z	0.00097	0.0937	Aux2	8x8x8	Z	0.00229	0.0670
Aux1	1x1x1	Z	0.00071	0.0690	Aux2	1x1x1	Z	0.00186	0.0487
Aux1	2x1x2	Y	0.00719	0.0273	Aux2	2x1x2	Y	0.00337	0.0553
Aux1	2x2x2	Y	0.00599	0.0419	Aux2	2x2x2	Y	0.00257	0.0766
Aux1	2x4x2	Y	0.00560	0.0398	Aux2	2x4x2	Y	0.00234	0.0724
Aux1	4x1x4	Y	0.00691	0.0292	Aux2	4x1x4	Y	0.00335	0.0571
Aux1	4x2x4	Y	0.00603	0.0448	Aux2	4x2x4	Y	0.00274	0.0765
Aux1	4x4x4	Y	0.00533	0.0409	Aux2	4x4x4	Y	0.00240	0.0708
Aux1	4x8x4	Y	0.00530	0.0403	Aux2	4x8x4	Y	0.00225	0.0696
Aux1	8x1x8	Y	0.00676	0.0298	Aux2	8x1x8	Y	0.00333	0.0575
Aux1	8x2x8	Y	0.00615	0.0446	Aux2	8x2x8	Y	0.00289	0.0737
Aux1	8x4x8	Y	0.00563	0.0418	Aux2	8x4x8	Y	0.00252	0.0787
Aux1	8x8x8	Y	0.00539	0.0432	Aux2	8x8x8	Y	0.00231	0.0798
Aux1	1x1x1	Y	0.00764	0.0251	Aux2	1x1x1	Y	0.00339	0.0509

Table 2 Size effects of auxetic cellular structures

It was known from analytical modeling that the two auxetic structures will exhibit different mechanical properties in both directions [22]. Auxetic 1 design should exhibit higher elastic modulus along the X/Y directions, while auxetic 2 design should exhibit similar elastic modulus along all three directions. From the results, both auxetic designs exhibit rather small size effects with elastic modulus. Both lateral and along-the-stress size effects stabilize when the number of unit cells is greater than 2-4, which agrees with the conclusions from previous studies with this structure [22]. On the other hand, the re-entrant auxetic structure exhibits more significant lateral size effects with maximum stress levels,

especially when the structure is loaded in the Z direction. Along-the-stress size effect for stress levels also appears to stabilize when the number of unit cells is greater than 2-4. It must be noted that the size effects for maximum stress is expected to correspond to the ultimate strength of the structures. Higher normalized maximum stress levels in the structures correspond to higher stress concentration factors in the structures and therefore lower ultimate strength, although additional studies are needed to quantify such relationships for each types of cellular geometries.

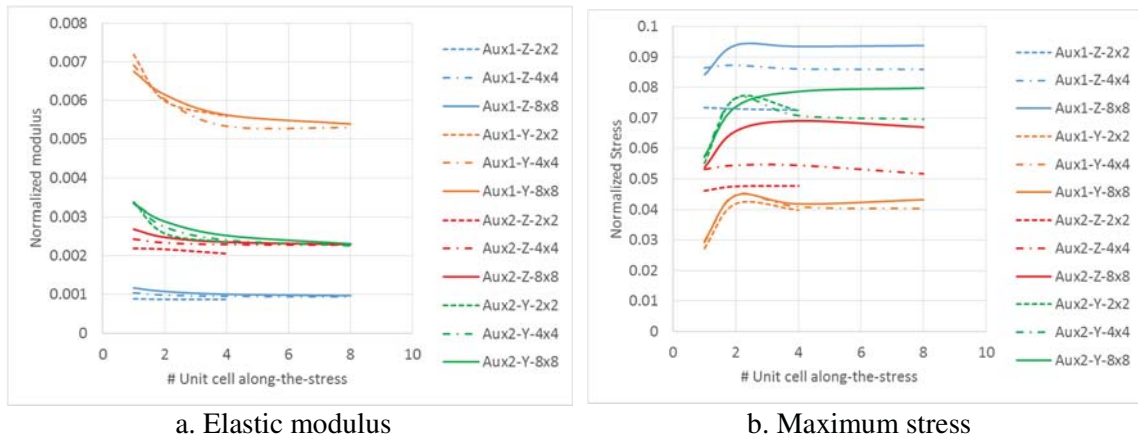


Fig.6 Size effects of re-entrant auxetic cellular designs

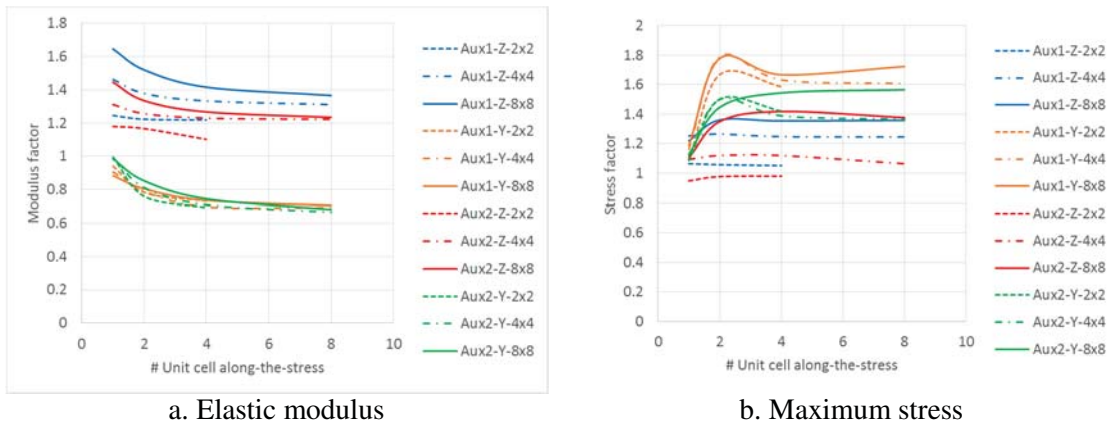


Fig.7 Relative size effects of re-entrant auxetic cellular designs compared to unit cell

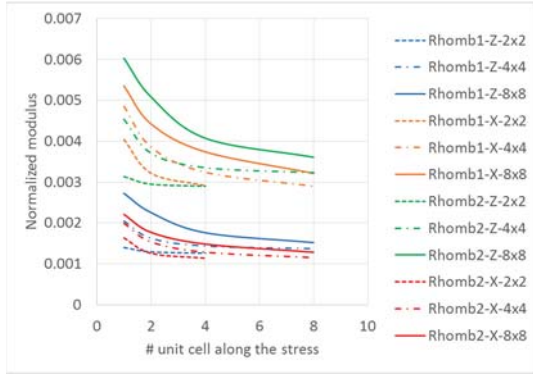
As the mechanical properties of the unit cell based cellular structures are often evaluated by unit cells, the mechanical characteristics of the re-entrant auxetic cellular structures with different numbers of unit cells were also compared with those of the unit cells. As shown in Fig.7, the size effects for relative modulus factors and stress factors, which correspond to the ratios between cellular structures and the unit cell for elastic modulus and maximum stress respectively. It naturally follows that these size effects also exhibit the same trends compared to the normalized properties as shown in Fig.6. Furthermore, additional conclusions can be drawn. When the auxetic structures are loaded along the Z direction, the elastic modulus of the structures are higher than those of the unit cells. On the other hand, when the auxetic structures are loaded along the X/Y direction, the resulting elastic modulus are lower than those of the unit cells. The auxetic structures also exhibit higher stress concentration when loaded in X/Y directions, although in general the size effects for

stress tend to result in higher stress concentration factors and therefore potentially lower strength.

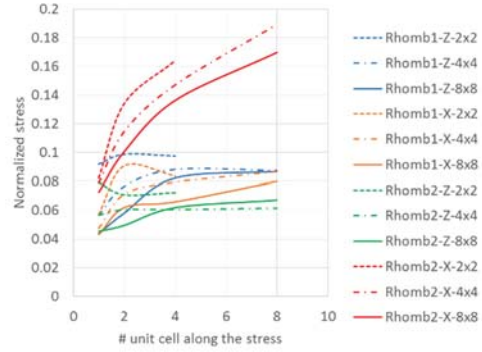
The size effects of the rhombic cellular structures are shown in Table 3 and Fig.8. From the results, for elastic modulus of both rhombic designs, the lateral size effect stabilizes when the numbers of unit cells are greater than 4-6, while the along-the-stress size effect appears to steadily become more significant at larger unit cell numbers. For maximum stress of both rhombic designs, the lateral size effects also appear to stabilize at threshold unit cell number of 4-6 except for rhombic 2 loaded along the X/Y directions. Furthermore, the lateral size effect for maximum stress also appears to be correlated to the overall aspect ratio of the unit cell geometries (i.e. the ratio between the dimension along the loading direction and the lateral dimension). For rhombic design higher aspect ratio appears to correspond to lower maximum stress levels and therefore lower stress concentration factors. One possible explanation is that higher aspect ratio corresponds to better strut alignment towards the loading direction and therefore reduced bending deformation when loaded.

Design	Pattern (X,Y,Z)	Loading dir.	Normalized elastic modulus (E/E _s)	Normalized max. stress (σ/σ_U)	Design	Pattern (X,Y,Z)	Loading dir.	Normalized elastic modulus (E/E _s)	Normalized max. stress (σ/σ_U)
Rhomb1	2x2x1	Z	0.00140	0.0918	Rhomb2	2x2x1	Z	0.00313	0.0791
Rhomb1	2x2x2	Z	0.00129	0.0987	Rhomb2	2x2x2	Z	0.00295	0.0707
Rhomb1	2x2x4	Z	0.00126	0.0976	Rhomb2	2x2x4	Z	0.00290	0.0722
Rhomb1	4x4x1	Z	0.00204	0.0566	Rhomb2	4x4x1	Z	0.00454	0.0566
Rhomb1	4x4x2	Z	0.00162	0.0765	Rhomb2	4x4x2	Z	0.00371	0.0603
Rhomb1	4x4x4	Z	0.00143	0.0882	Rhomb2	4x4x4	Z	0.00335	0.0604
Rhomb1	4x4x8	Z	0.00137	0.0875	Rhomb2	4x4x8	Z	0.00323	0.0613
Rhomb1	8x8x1	Z	0.00272	0.0438	Rhomb2	8x8x1	Z	0.00603	0.0453
Rhomb1	8x8x2	Z	0.00225	0.0580	Rhomb2	8x8x2	Z	0.00508	0.0495
Rhomb1	8x8x4	Z	0.00176	0.0822	Rhomb2	8x8x4	Z	0.00407	0.0618
Rhomb1	8x8x8	Z	0.00152	0.0868	Rhomb2	8x8x8	Z	0.00361	0.0670
Rhomb1	1x1x1	Z	0.00117	0.0508	Rhomb2	1x1x1	Z	0.00262	0.0400
Rhomb1	2x1x2	Y	0.00403	0.0570	Rhomb2	2x1x2	Y	0.00163	0.0820
Rhomb1	2x2x2	Y	0.00321	0.0906	Rhomb2	2x2x2	Y	0.00126	0.1341
Rhomb1	2x4x2	Y	0.00292	0.0835	Rhomb2	2x4x2	Y	0.00114	0.1642
Rhomb1	4x1x4	Y	0.00485	0.0473	Rhomb2	4x1x4	Y	0.00199	0.0787
Rhomb1	4x2x4	Y	0.00385	0.0710	Rhomb2	4x2x4	Y	0.00153	0.1144
Rhomb1	4x4x4	Y	0.00324	0.0793	Rhomb2	4x4x4	Y	0.00128	0.1470
Rhomb1	4x8x4	Y	0.00290	0.0865	Rhomb2	4x8x4	Y	0.00114	0.1894
Rhomb1	8x1x8	Y	0.00535	0.0430	Rhomb2	8x1x8	Y	0.00221	0.0726
Rhomb1	8x2x8	Y	0.00422	0.0618	Rhomb2	8x2x8	Y	0.00177	0.1006
Rhomb1	8x4x8	Y	0.00374	0.0658	Rhomb2	8x4x8	Y	0.00148	0.1362
Rhomb1	8x8x8	Y	0.00321	0.0799	Rhomb2	8x8x8	Y	0.00128	0.1697
Rhomb1	1x1x1	Y	0.00292	0.0534	Rhomb2	1x1x1	Y	0.00113	0.1013

Table 3 Size effects of rhombic cellular structures



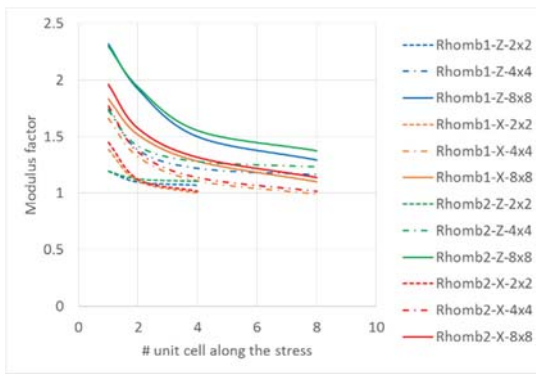
a. Elastic modulus



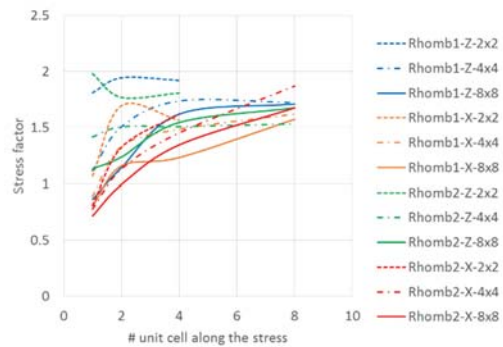
b. Maximum stress

Fig.8 Size effects of rhombic cellular designs

Fig.9 shows the relative size effects of rhombic cellular structures compared to unit cells. When the number of unit cell is 1 or 2 along the stress directions, the rhombic structure appears to exhibit the optimal combination of highest elastic modulus and lowest stress concentration. Lateral size effects also appear to enhance such effects, as the rhombic structures with 8x8 lateral patterns exhibit the most significant performance improvement.



a. Elastic modulus



b. Maximum stress

Fig.9 Relative size effects of rhombic cellular designs compared to unit cell

The size effects of the octet-truss structures are shown in Table 4 and Fig.10. Due to the structural symmetry of the octet-truss unit cell, only one geometrical design and loading direction combination was studied. For octet-truss structures the lateral size effects appear to stabilize when unit cell number is greater than 8, while the along-the-stress size effect appears to be less significant. The relative size effects as shown in Fig.11 also exhibit the same trend. For octet-truss structures the elastic modulus is generally lower than that of the unit cell, and the stress concentration factor quickly rises to over 1.5 whenever patterns with multiple unit cells are present. For larger octet-truss structures with more than 8 unit cells in each directions, the stress concentration factor indicates that the initial failure strength could be reduced by over 60%.

Design	Pattern (X,Y,Z)	Loading dir.	Normalized elastic modulus (E/E_s)	Normalized max. stress (σ/σ_U)
Oct1	2x2x1	Z	0.00504	0.0327
Oct1	2x2x2	Z	0.00426	0.0434
Oct1	2x2x4	Z	0.00384	0.0582
Oct1	4x4x1	Z	0.00516	0.0357
Oct1	4x4x2	Z	0.00454	0.0469
Oct1	4x4x4	Z	0.00405	0.0602
Oct1	4x4x8	Z	0.00382	0.0653
Oct1	8x8x1	Z	0.00525	0.0378
Oct1	8x8x2	Z	0.00483	0.0439
Oct1	8x8x4	Z	0.00433	0.0566
Oct1	8x8x8	Z	0.00386	0.0878
Oct1	1x1x1	Z	0.00501	0.0331

Table 4 Size effects of octet-truss cellular structures

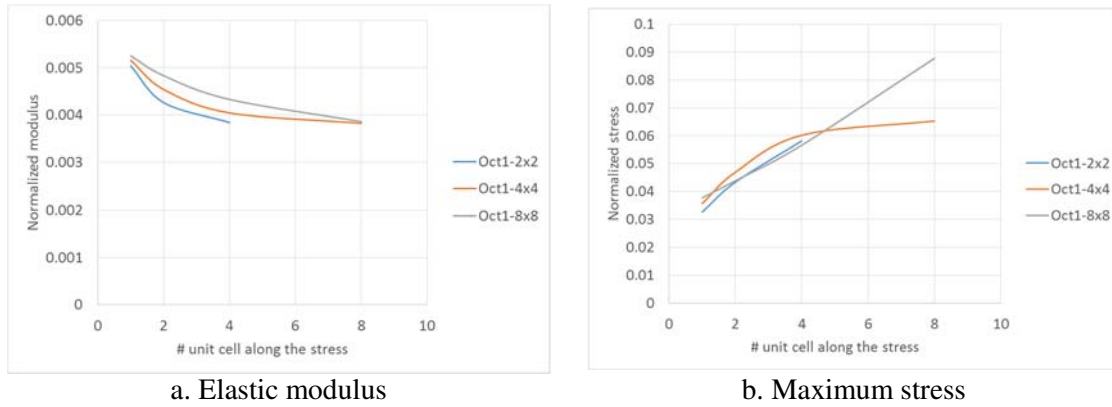


Fig.10 Size effects of octet-truss cellular designs

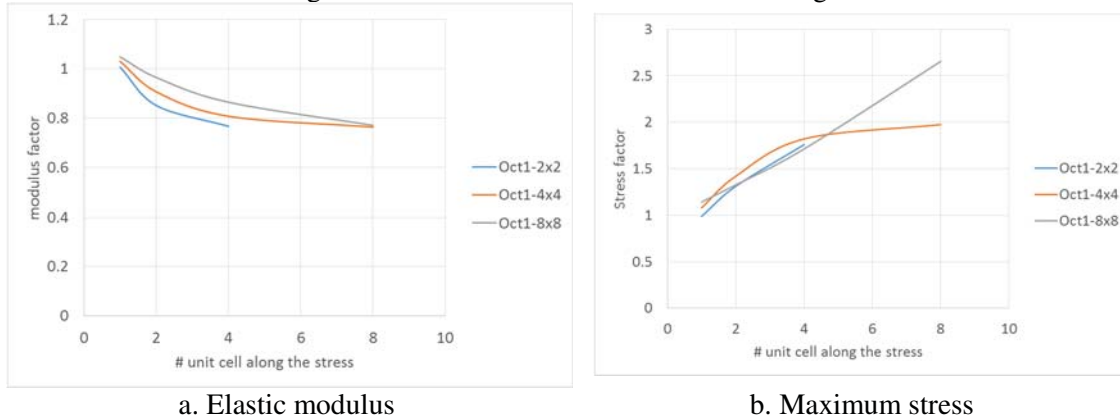


Fig.11 Relative size effects of octet-truss cellular designs compared to unit cell

The size effects of BCC lattice cellular structures are shown in Table 5 and Fig.12. As the BCC2 lattice design exhibit identical geometries along all three directions, only one loading direction was studied. In general the BCC lattice exhibits significant size effects in both lateral and along-the-stress directions. In addition, such size effects appear to be strongly correlated to the number of unit cells in the directions normal to the direction of interest. For example, BCC lattice designs with 8x8 lateral unit cell patterns exhibit strong size effect at unit cell number of 8, while for all the designs with 4x4 and 2x2 lateral unit

cell patterns, the size effects stabilize at unit cell number of 4 and 2 respectively. The same correlation has been demonstrated previously, and it is likely caused by the specific stress concentration patterns with the compression of BCC lattice structures [11].

Design	Pattern (X,Y,Z)	Loading dir.	Normalized elastic modulus (E/E _s)	Normalized max. stress (σ/σ _U)	Design	Pattern (X,Y,Z)	Loading dir.	Normalized elastic modulus (E/E _s)	Normalized max. stress (σ/σ _U)
BCC1	2x2x1	Z	0.001245	0.0877	BCC2	2x2x1	Z	0.00222	0.0607
BCC1	2x2x2	Z	0.00079	0.1981	BCC2	2x2x2	Z	0.00079	0.1981
BCC1	2x2x4	Z	0.00073	0.1797	BCC2	2x2x4	Z	0.00073	0.1797
BCC1	4x4x1	Z	0.00191	0.0687	BCC2	4x4x1	Z	0.00284	0.0525
BCC1	4x4x2	Z	0.00145	0.1144	BCC2	4x4x2	Z	0.00145	0.1142
BCC1	4x4x4	Z	0.00094	0.2126	BCC2	4x4x4	Z	0.00126	0.1326
BCC1	4x4x8	Z	0.00077	0.1845	BCC2	4x4x8	Z	0.00098	0.1408
BCC1	8x8x1	Z	0.00234	0.0565	BCC2	8x8x1	Z	0.00308	0.0443
BCC1	8x8x2	Z	0.00203	0.0818	BCC2	8x8x2	Z	0.00258	0.0649
BCC1	8x8x4	Z	0.00153	0.1171	BCC2	8x8x4	Z	0.00192	0.0878
BCC1	8x8x8	Z	0.00101	0.2104	BCC2	8x8x8	Z	0.00124	0.1580
BCC1	1x1x1	Z	0.00066	0.1077	BCC2	1x1x1	Z	0.00104	0.0712
BCC1	2x1x2	Y	0.00404	0.0364					
BCC1	2x2x2	Y	0.00185	0.1137					
BCC1	2x4x2	Y	0.00162	0.1135					
BCC1	4x1x4	Y	0.00550	0.0378					
BCC1	4x2x4	Y	0.00378	0.0527					
BCC1	4x4x4	Y	0.00215	0.0929					
BCC1	4x8x4	Y	0.00170	0.1102					
BCC1	8x1x8	Y	0.00628	0.0355					
BCC1	8x2x8	Y	0.00567	0.0503					
BCC1	8x4x8	Y	0.00382	0.0657					
BCC1	8x8x8	Y	0.00225	0.1057					
BCC1	1x1x1	Y	0.00154	0.0755					

Table 5 Size effects of BCC lattice cellular structures

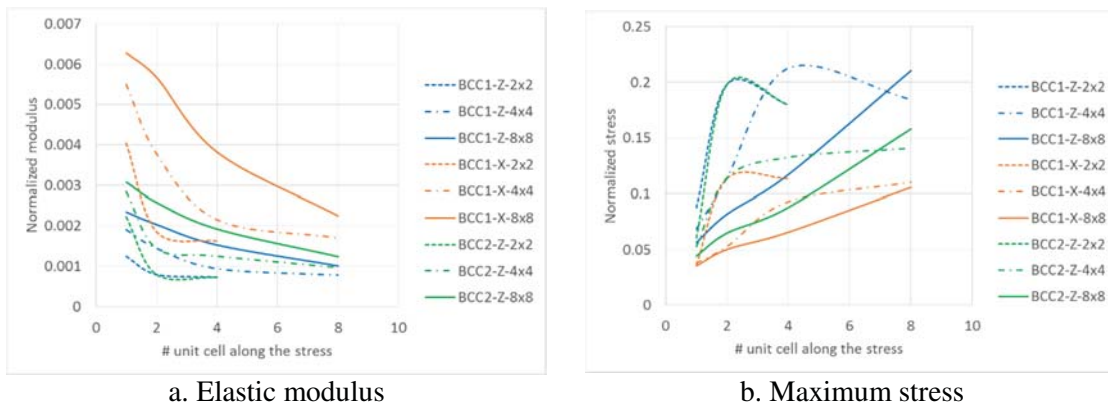


Fig.12 Size effects of BCC lattice cellular structures

The relative size effects of the BCC lattice are shown in Fig.13. Again similar size effect trends were observed for modulus and maximum stress. When the number of unit cells is

sufficiently large, the elastic modulus of the BCC lattice converges to that of the unit cell, which could be potentially utilized during the design. On the other hand, the stress concentration factors appear to achieve maximum magnitude when the numbers of unit cells in the lateral directions are identical to the number of unit cells along the loading direction.

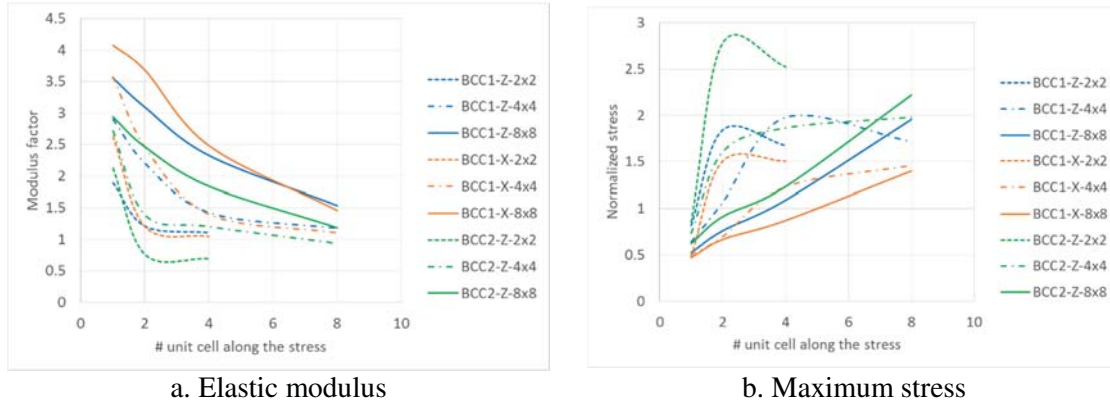


Fig.13 Relative size effects of BCC lattice cellular designs compared to unit cell

For all the cellular designs, it can be seen that cellular patterns that are commonly seen for sandwich panel structures, i.e. large lateral unit cell patterns and small number of layers of unit cells along the thickness directions, appear to exhibit the optimal mechanical properties when subjected to normal compressive loading. In general, re-entrant auxetic structures exhibit significantly less size effects compared to the other structures, which might be partially contributed to their unique negative Poisson's ratio characteristics. On the other hand, both octet-truss and BCC lattice exhibit most significant size effects. Also, in general lateral size effects tend to strengthen the structures, while along-the-stress size effects generally reduces the structural performance.

Conclusions

In this paper, simulation based studies were carried out to evaluate the size effects of multiple unit cell cellular designs including re-entrant auxetic, rhombic, octet-truss and BCC lattice. It was found that for all the cellular designs, lateral size effects tend to increase the mechanical properties of the cellular structures while along-the-stress size effects tend to decrease them. As a result, it was concluded that sandwich panel designs with large lateral numbers of unit cells and few layers of unit cells along the thickness directions might possess optimal properties when subjected to compressive loading. Among the four cellular structures, the auxetic structure exhibits smallest size effects, while octet-truss and BCC lattice exhibit most significant size effects. On the other hand, the size effects for both auxetic and BCC lattice cellular structures appear to be highly predictable, therefore could potentially be accounted for during the cellular structure modeling. The deformation mechanism does not appear to play significant role in determining size effects, while unit cell dimensional aspect ratio might contribute to different size effects for certain cellular designs such as rhombic.

Acknowledgement

This work was partially supported by Office of Naval Research (ONR) grant #N00014-16-1-2394. The author would like to acknowledge the support of Rapid Prototyping Center (RPC) at University of Louisville.

Reference

- [1] V. S. Deshpande, N. A. Fleck, M. F. Ashby. Effective properties of the octet-truss lattice material. *Journal of Mechanics and Physics of Solids*. 49(2001): 1747-1769.
- [2] C. Yan, L. Hao, A. Hussein, D. Raymont. Evaluations of cellular lattice structures manufactured using selective laser melting. *International Journal of Machine Tools and Manufacture*. 62(2012): 32-38.
- [3] R. Gumruk, R. A. W. Mines. Compressive behaviour of stainless steel micro-lattice structures. *International Journal of Mechanical Sciences*. 68(2013): 125-139.
- [4] L. Yang, O. Harrysson, H. West, D. Cormier. Compressive properties of Ti-6Al-4V auxetic mesh structures made by electron beam melting. *Acta Materialia*. 60(2012): 3370-3379.
- [5] H. V. Wang, S. R. Johnston, D. W. Rosen. Design of a graded cellular structure for an acetabular hip replacement component. *Proceedings of 17th International Solid Freeform Fabrication (SFF) Symposium*. Austin, Texas, USA, 2006.
- [6] A. G. Evans, J. W. Hutchinson, M. F. Ashby. Multifunctionality of cellular metal systems. *Progress in Materials Science*. 43(1999): 171-221.
- [7] M. F. Ashby. The properties of foams and lattices. *Philosophical Transactions of The Royal Society A*. 364(2006): 15-30.
- [8] L. Yang, O. Harrysson, D. Cormier, H. West, H. Gong, B. Stucker. Metal cellular structures with additive manufacturing: design and fabrication. *Journal of Materials*. 67(2015), 3:608-615.
- [9] S. A. Khanoki, D. Pasini. Multiscale design and multiobjective optimization of orthopedic hip implants with functionally graded cellular material. *Journal of Biomechanical Engineering*. 134(2012): 031004.
- [10] L. E. Murr, S. M. Gaytan, F. Medina, H. Lopez, E. Martinez, B. I. Machado, D. H. Hernandez, L. Martinez, M. I. Lopez, R. B. Wicker, J. Bracke. Next-generation biomedical implants using additive manufacturing of complex, cellular and functional mesh arrays. *Philosophical Transactions of The Royal Society A*. 368(2010): 1999-2032.
- [11] L. Yang. Experimental-assisted design development for an octahedral cellular structure using additive manufacturing. *Rapid Prototyping Journal*. 21(2015), 2: 168-176.
- [12] C. Yan, L. Hao, A. Hussein, D. Raymont. Evaluations of cellular lattice structures manufactured using selective laser melting. *International Journal of Machine Tools & Manufacture*. 62(2012): 32-38.
- [13] J. F. Rakow, A. M. Waas. Size effects and the shear response of aluminum foam. *Mechanics of Materials*. 37(2005): 69-82.
- [14] E. W. Andrews, G. Gioux, P. Onck, L. J. Gibson. Size effects in ductile cellular solids. Part II: experimental results. *International Journal of Mechanical Sciences*. 43(2001): 701-713.

- [15] O. Kesler, L. J. Gibson. Size effects in metallic foam core sandwich beams. *Materials Science and Engineering A*. 326(2002): 228-234.
- [16] G. Dai, W. Zhang. Size effects of effective Young's modulus for periodic cellular materials. *Science in China Series G: Physics, Mechanics and Astronomy*. 52(2009), 8: 1262-1270.
- [17] P. R. Onck, E. W. Andrews, L. J. Gibson. Size effects in ductile cellular solids. Part I: modeling. *International Journal of Mechanical Sciences*. 43(2001): 681-699.
- [18] C. Tekoglu, P. R. Onck. Size effects in the mechanical behavior of cellular materials. *Journal of Materials Science*. 40(2005): 5911-5917.
- [19] L. Yang, O. Harrysson, H. West, D. Cormier. Modeling of uniaxial compression in a 3D periodic re-entrant lattice structure. *Journal of Materials Science*. 48(2013): 1413-1422.
- [20] O. L. A. Harrysson, O. Cansizoglu, D. J. Marcellin-Little, D. R. Cormier, H. A. West II. Direct metal fabrication of titanium implants with tailored materials and mechanical properties using electron beam melting technology. *Materials Science and Engineering C*. 28(2008): 366-373.
- [21] O. Cansizoglu, D. Cormier, O. Harrysson, H. West, T. Mahale. An Evaluation of Non-Stochastic Lattice Structures Fabricated Via Electron Beam Melting. *Proceedings of the 17th International Solid Freeform Fabrication (SFF) Symposium*. Austin, Texas, USA, 2006.
- [22] L. Yang, O. Harrysson, H. West, D. Cormier. Mechanical properties of 3D re-entrant honeycomb auxetic structures realized via additive manufacturing. *International Journal of Solids and Structures*. 69-70(2015): 475-490.